

MASSACHUSETTS INSTITUTE OF TECHNOLOGY

3.014 Materials Laboratory  
Fall 2006

**LABORATORY 4: Module  $\beta_2$**

*Mechanical Properties of Alkali Borate Glasses*

©2006 Linn W. Hobbs

Instructor: Professor Linn W. Hobbs

**Objectives**

Experience the glass transition through observing temperature dependence of viscosity  
Observe change in glass transition effected by changes in glass composition  
Relate thermal, spectroscopic and diffraction features to glass structure

**Tasks**

Draw sodium borate glass fibers from prepared melts  
Measure speed of sound in borate glass fibers using ultrasonic pulse transit  
Determine load-displacement curves for borate glass fibers in 3-point bend tests  
Deduce critical flaw size and fracture toughness of borate glass fibers

**Materials**

Sodium carbonate powder ( $\text{Na}_2\text{CO}_3$ ), 250g  
Boric acid powder ( $\text{H}_3\text{BO}_3$ ), 500g  
8 Alumina crucibles, 50ml  
8 Silica glass rods, 4-mm diameter

**Introduction**

A *GLASS* is, formally, a solid that solidifies without a well-defined melting point—defined as a singular temperature at which there occurs a discontinuous change in a physical property, for example specific volume, during transition between a liquid state and its corresponding solid state—but instead exhibits a continuous change in that property over a range of temperature. Glasses tend to inherit their atomic-scale structures from those of the liquids from which they evolve by cooling, and their structural arrangements are therefore necessarily less-ordered than those of corresponding crystalline arrangements. Such glassy arrangements are often termed *amorphous*, though formally again what is meant by this term is lack of the long-range translational and rotational regularity that characterize crystalline arrangements. All “amorphous” atom arrangements do not necessarily exhibit a formal *glass transition*, though many do. Good

examples are 1) vitreous silica [ $\text{SiO}_2$ ] (also known as “fused quartz” because in its production crystalline quartz is melted, then cooled rapidly enough to ensure that crystallization does not take place); 2) soda-lime glass (“window glass”) formed by dissolving sodium and calcium oxides into a silica melt and cooling; 3) aluminoborosilicate labware glasses like Pyrex.<sup>®</sup>

Chemical bonding of atoms—whether ionic, covalent or metallic in character—governs the coordination of other atoms around any given atom in a solid. For metallic and ionic solids, atom or ion sizes are a principal factor in determining coordination, which tends to be high (usually between 6 and 12). The orbital geometries and directivity of covalent bonds occasion rather lower coordination (typically 2 to 4). The preferred coordination is clearly critical in deciding the crystal structure adopted in crystalline solids. The coordination established by chemical bonding in less regular atomic arrangements—for example, glasses—is often similar or identical to that in crystals and is equally important in deciding the structure of non-crystalline solids. The connectivity of coordinated groups of atoms in turn governs many mechanical responses of the non-crystalline solid. This experiment explores the consequences—for the propagation of mechanical vibrations, for elastic deformation response, and for fracture strength—of changes in the nature of the network bonding and structure in alkali borate glasses.

Lacking the “crutch of periodicity” that enables even complicated inorganic crystal structures to be described by a few, or a few tens of, atoms in a uniform unit cell, glass structures resist description and are still partly a matter for speculation. One useful approach, first addressed by the noted American crystal chemist William H. Zachariasen in 1932 in the only paper he published on glass structure,<sup>1</sup> starts with connectivity—which atoms are likely to be connected to which other atoms—and seeks empirically to construct a network that resists shear (thus distinguishing it from a liquid), lacks long-range translational and orientational regularity (thus distinguishing it from a crystalline arrangement), and can be extended indefinitely. Zachariasen chose as his paradigm vitreous silica, a three-dimensional oxide network glass, in which silicon atoms are invariably surrounded by four oxygen atoms, forming  $[\text{SiO}_4]$  tetrahedral units that connect to each other by sharing common oxygen atoms at each of their four vertices. But in the simpler heuristic depiction he chose to illustrate, Zachariasen used  $[\text{AO}_3]$  equilateral triangular units, sharing each of their three vertex oxygens with other triangular units in two dimensions.

It is, of course, trivial to extend a network of corner-sharing triangles indefinitely in two dimensions if the triangles are oriented identically to form a hexagonal crystalline network. But Zachariasen found that he could extend such a network seemingly indefinitely even if the triangles were *randomly* rotated with respect to each other (random A-O-A angle). His model, later coined the “continuous random network” by MIT X-ray crystallographer and physics professor Bertram E. Warren<sup>2</sup> (MIT SB ’24, SM ’25, DSc ’29) who studied glass structure by X-ray diffraction in the 1950’s, has become the standard textbook illustration for network glass structure (even though the model was not proven extendable to three dimensions until the 1990’s).

---

<sup>1</sup>W. H. Zachariasen, *J. Amer. Chem. Soc.* **54** (1932) 3841-3851.

<sup>2</sup>B. E. Warren, *J. Amer. Ceram. Soc.* **17** (1934) 249.

## **Topology and Rigidity**

A more rigorous approach to description of glass structure employs the mathematics of network topology<sup>3</sup> (much explored in the last two decades because of the importance of pervasive computer networks) and analyzes continuous closed paths, called *rings*, in a network of connected *polytopes* (geometrical coordination units, like the  $[\text{SiO}_4]$  tetrahedra or  $[\text{AO}_3]$  triangles of the last two examples). Moreover, a topological approach can explain why solids form non-crystalline structures at all. The reason is related to rigidity theory<sup>4</sup>, a formal exploration of which was first undertaken by James Clerk Maxwell<sup>5</sup>, the mid-19<sup>th</sup> century Cambridge University physicist whose compact formulation of the laws governing electromagnetic phenomena are now known as Maxwell's relations. Maxwell discovered that rigid connected structures, like a bridge truss, derive their stability from the fact that the degrees of freedom at the connection points of the structure (3 degrees of freedom in three-dimensions) are exceeded by the constraints imposed on that freedom by the connections to other parts of the structure. Ceramists Alfred R. Cooper (MIT Ph.D. '60 and former Course III professor) and his former student Prabat K. Gupta (now a professor at Ohio State University) codified these constraints for arbitrary polytopes (rods, triangles, tetrahedral, octahedral, cubes...) and connectivity motifs (vertex-sharing, edge-sharing, face-sharing) and established a parameter called *structural freedom f* to describe the excess of freedoms over constraints, which was found to correlate with glass-forming ability<sup>6</sup> and amorphizability<sup>4</sup>. Their analysis yields

$$f = d - C\{\delta - [\delta(\delta+1)/2V]\} - (d-1)(Y/2) - [(p-1)d - (2p-3)](Z/p) \quad (1)$$

where  $d$  is dimension of the stucture (1-, 2- or 3-dimensional),  $\delta$  is the dimension of the polytope,  $C$  (the “connectivity”) is the number of polytopes with  $V$  vertices meeting at a vertex,  $Y$  is the fraction of vertices which participate in sharing of edges (defined by 2 adjacent vertices), and  $Z$  is the fraction of vertices that participate in sharing of  $p$ -sided faces. As an instructive example, MgO (with the rocksalt structure) is comprised of  $[\text{MgO}_6]$  octahedra sharing each of their six edges with five other adjacent octahedra ; the parameters

---

<sup>3</sup>L. W. Hobbs, C. E. Jesurum, V. Pulim and B. Berger, “Local topology of silica networks,” *Philos. Mag. A* **78** (1998) 679-711. L. W. Hobbs, C. Esther Jesurum and Bonnie Berger, “The topology of silica networks,” Chapter 1 in: *Structure and Imperfections in Amorphous and Crystalline Silica*, ed. J.-P. Duraud, R. A. B. Devine and E. Dooryhee (John Wiley & Sons, London, 2000) pp. 1-47. Linn W. Hobbs and Xianglong Yuan, “Topology and Topological Disorder in Silica,” in: *Defects in SiO<sub>2</sub> and Related Dielectrics: Science and Technology*, ed. G. Pacchioni, L. Skuja and D. L. Griscom (Kluwer, Dordrecht, Netherlands, 2000) pp. 37-71.

<sup>4</sup>Linn W. Hobbs, C. Esther Jesurum and Bonnie Berger, “Rigidity constraints in the amorphization of singly- and multiply-polytopic structures,” in: *Rigidity Theory and Applications*, ed. P. M. Duxbury and M. F. Thorpe (Plenum Press, New York, 1999) 191-216.

<sup>5</sup>J. C. Maxwell, *Philos. Mag.* **27** (1864) 294.

<sup>6</sup>P. K. Gupta and A. R. Cooper, *J. Non-Crystalline Solids* **123** (1990) 14. P. K. Gupta, *J. Amer. Ceram. Soc.* **76** (1993) 1088.

for (1) are ( $d = 3$ ,  $\delta = 3$ ,  $V = 6$ ,  $C = 6$ ,  $Y = 1$ ,  $Z = 0$ ) and yield  $f = -10$ . The large negative value of  $f$  means that MgO is extraordinarily *overconstrained* and proves virtually impossible to amorphize: it always solidifies or self-assembles into the crystalline state and will retain that structure without rearrangement even when a large fraction of the interionic connections are missing. By contrast, SiO<sub>2</sub> comprises [SiO<sub>4</sub>] tetrahedra sharing each of their four vertices with another tetrahedron ( $d = 3$ ,  $\delta = 3$ ,  $V = 4$ ,  $C = 2$ ,  $Y = 0$ ,  $Z = 0$ ) and yields  $f = 0$ . SiO<sub>2</sub> structures are therefore only marginally constrained, and breaking only a small number of bonds renders the structure floppy and able to rearrange and rebond into many alternative arrangements, most of them non-crystalline, with only small differences in internal energy from those of crystalline silica structures. Silica, with  $f = 0$ , is the archetypal glass former.

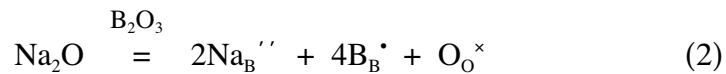
### ***Borate Glasses***

SiO<sub>2</sub> forms [SiO<sub>4</sub>] tetrahedra because the single filled 3s and two half-filled 3p Si orbitals (containing a total of 4 electrons) hybridize to form four “sp<sub>3</sub> bonds,” each containing a single unpaired electron, pointing to the corners of a tetrahedron at mutual angles of about 107°. [The silicon atom (atomic number Z = 14) electronic structure is: 1s<sup>2</sup> 2s<sup>2</sup> 2p<sup>6</sup> 3s<sup>2</sup> 3p<sub>x</sub><sup>1</sup> 3p<sub>y</sub><sup>1</sup>.] Each of the four “sp<sub>3</sub> bonds” reaches out to one of the two half-filled oxygen 2p orbitals in a neighboring oxygen atom, each containing a single electron [oxygen (Z = 8) electronic structure: 1s<sup>2</sup> 2s<sup>2</sup> 2p<sub>z</sub><sup>2</sup> 2p<sub>x</sub><sup>1</sup> 2p<sub>y</sub><sup>1</sup>] to form an Si-O “bond” containing a pair of electrons. Thus, each Si is tetrahedrally coordinated by four O atoms (in [SiO<sub>4</sub>] tetrahedral polytopes) and each O (the other half-filled O 2p orbital reaching out to a second Si) is coordinated by two Si atoms, with an Si-O-Si angle that can take on values between about 120° and 180°. Carbon (Z = 6, electronic structure: 1s<sup>2</sup> 2s<sup>2</sup> 2p<sub>x</sub><sup>1</sup> 2p<sub>z</sub><sup>1</sup>) analogously hybridizes the single filled 2s and two half-filled 2p orbitals to form the strong tetrahedral “sp<sub>3</sub>” bonds in diamond; but it can also hybridize the 2s<sup>2</sup> orbital electrons with a single electron from one 2p orbital to form three “sp<sub>2</sub>” bonds at 120° holding together the planar hexagonal layers of graphite, the remaining 2p<sub>z</sub> orbital electron available to effect weaker interlayer bonding.

Boron (atomic number Z = 5, electronic structure: 1s<sup>2</sup> 2s<sup>2</sup> 2p<sub>x</sub><sup>1</sup>) can perform the same trick. Hybridization of the filled 2s and half-filled single 2p<sub>x</sub> orbital yields three “sp<sub>2</sub>” bonds at 120°, so that boron combines with oxygen as [BO<sub>3</sub>] triangular polytopes which share corner oxygens to form two-dimensional network sheets with composition B<sub>2</sub>O<sub>3</sub> (with *no* O 2p orbital electron left over to effect bonding between sheets, as in graphite). This structure is exactly the two-dimensional Zachariasen model, for which  $d = 2$ ,  $\delta = 2$ ,  $V = 3$ ,  $C = 2$  and  $f = 0$ . In three dimensions,  $d = 3$ , and structural freedom for B<sub>2</sub>O<sub>3</sub> is increased to  $f = +1$ ; thus, in the three-dimensional solid, a certain floppiness of the network is expected, or at least it is not expected to exhibit a high stiffness. As expected, B<sub>2</sub>O<sub>3</sub> is a facile glass former and is, in fact, difficult to retain in crystalline form. There is evidence that about 70% of the [BO<sub>3</sub>] triangles arrange themselves into [B<sub>3</sub>O<sub>6</sub>] super-structural units called *bороxyl rings*, each бороxyl unit comprising three triangles in a 3-ring. The superstructure units are connected to other [BO<sub>3</sub>] triangles or other бороxyl rings through three common oxygens per unit, just as are [BO<sub>3</sub>] triangles, so the бороxyl units are just larger triangular polytopes, and the fundamental topology is not changed.

Because glasses undergoing a glass transition change continuously from a liquid (of low viscosity) to a solid (of effectively infinite viscosity) when cooled, the point of “solidification” is defined operationally as when the viscosity reaches a critical value (taken as  $10^{13}$  Pa s) at a temperature called the glass transition temperature ( $T_g$ ). If an alkali (or alkaline earth) oxide, like  $\text{Na}_2\text{O}$  is added to  $\text{SiO}_2$ , it has been known for at least four millennia that the viscosity of silica glass is substantially reduced, so that it can be poured or worked (viscosities of  $10^3$ - $10^7$  Pa s) at temperatures as low as  $700^\circ \text{C}$ , easily accessible to ancient pyrotechnologies. This phenomenon is the basis of the soda-lime silicate glass compositions (16mol% $\text{Na}_2\text{O}$ -10mol% $\text{CaO}$ -74mol% $\text{SiO}_2$ ) still in common use today—for beer bottles and window glass, for example. The explanation is that the large, highly ionic alkali or alkaline earth ions prefer to be coordinated by as many oxygen atoms as possible; this coordination can only be achieved if network Si-O bonds are broken, leaving some oxygens connected to the network through only one, not two bonds (these are called “non-bridging oxygens,” or NBOs), each NBO being left with an electron in a “dangling” 2p orbital that can interact strongly with positively charged alkali ions, which then distribute themselves in regions of locally high NBO density. In fact,  $\text{Na}_2\text{O}$  is readily soluble in  $\text{SiO}_2$  because Na ion goes from 4-fold coordination by oxygen in the anti-fluorite structure of  $\text{Na}_2\text{O}$  to higher average oxygen coordination in the sodium silicate glass. The resulting structure is called a “modified random network” and is less connected, exhibiting lowered viscosity and stiffness at a given temperature and a reduction of  $T_g$  from  $\sim 1250^\circ \text{C}$  in pure silica glass to  $\sim 600^\circ \text{C}$  in soda-lime silicate glass incorporating these two network modifier cations.

Soda can also be dissolved into  $\text{B}_2\text{O}_3$ , but the initial result is quite different: the glass stiffens and exhibits a minimum in the thermal expansion coefficient around 16mol%  $\text{Na}_2\text{O}$ , exactly the opposite of what happens with soda dissolved into silica. This is known as the “boron anomaly,” an explanation of which is that the addition of  $\text{Na}^+$  ions converts vertex-sharing  $[\text{BO}_3]$  triangles to vertex-sharing  $[\text{BO}_4]$  tetrahedra. On a formally “ionic” model, dissolution of soda into  $\text{B}_2\text{O}_3$  can be represented as



where ‘ represents a negative charge, ‘ a positive charge, and  $^{\times}$  neutrality with respect to the usual electrostatic expectation at a given site.  $\text{B}^{3+}$  is in effect oxidized to a  $\text{B}^{4+}$  valence state, though on a covalent model this is not quite how it happens. Instead, an oxygen ion (electronic configuration:  $1s^2 2s^2 2p^6$ ), introduced to the network and coordinated to a stabilizing near-neighbor  $\text{Na}^+$  ion, effectively contributes an electron to a second  $2p_y$  orbital in each of two adjacent boron atoms, which in turn hybridize the filled  $2s^2$  and resulting half-filled  $2p_x^1$  and  $2p_y^1$  orbitals into four tetrahedral “ $sp_3$  bonds” extending out to four tetrahedrally coordinating oxygen atoms (each oxygen then has the atom electronic configuration:  $1s^2 2s^2 2p_z^2 2p_x^1 2p_y^1$ ). One mole of  $\text{Na}_2\text{O}$  thus converts four moles of  $[\text{BO}_3]$  triangles to  $[\text{BO}_4]$  tetrahedra, and a triangular  $f = +1$  network into a tetrahedral  $f = 0$  network, with a net gain in rigidity. If no other network changes occurred, conversion would be theoretically complete for the composition  $0.5\text{Na}_2\text{O}\bullet\text{B}_2\text{O}_3$ —equivalent to composition  $\text{Na}_2\text{B}_4\text{O}_7$  (anhydrous borax) which, by analogy to Na-silicate glasses, should comprise a  $\text{Na}^+$ -ion-stabilized fully tetrahedral

network). In reality, the  $[BO_4]$  tetrahedral unit occurs in several intermediate configurations based on arrangements of  $[BO_3]$  and  $[BO_4]$  polytopes found in crystalline alkali borate structures<sup>7</sup>—e.g the  $[B_3O_7]$  triborate and  $[B_5O_{10}]$  pentaborate units each containing one  $[BO_4]$  tetrahedron per unit, and the  $[B_4O_{10}]$  diborate unit containing two linked  $[BO_4]$  tetrahedra per unit. The concentration of single  $[BO_4]$  tetrahedra, however accommodated, rises continuously with increasing alkali content up to about 30mol%<sup>8</sup> and then diminishes as the isolated tetrahedra are replaced in turn by diborate groups and a more extensive tetrahedral network at higher  $[BO_4]$  density.<sup>9</sup> (It turns out that the anomalous expansion coefficient minimum at 16mol% Na<sub>2</sub>O content may arise from an allied but distinguishable phenomenon of phase separation on a nanometer scale into alkali-rich and alkali-poor compositions.<sup>10</sup>)

### ***Sound and Strain***

The bonding constraints in a solid act as springs with a characteristic stiffness because the interatomic forces act elastically until the bonds are ruptured. These atomic springs act in concert, so in general the more topologically overconstrained the structure is for a given bond strength, the stiffer the structure. Just as a spring responds to an applied force by extending or contracting, so a solid responds to an applied force by deforming. If the deformation is reversibly proportional to the applied force, the response is termed *linearly elastic*.

**1. Linear elasticity.**<sup>11</sup> Consider a volume element located at some point in the interior of a solid body, with a unit normal  $\mathbf{n}$  associated with a unit surface area of the volume element. Suppose force  $\mathbf{F}$ , with components  $F_i$  along three principal axes ( $i = 1,2,3$ ), acts on this volume element. The force can then be described by the equation

$$\mathbf{F} = \underline{\sigma} \cdot \mathbf{n}. \quad (3)$$

The elements of the force  $\mathbf{F}$  are

$$F_i = \sum_{j=1}^3 \sigma_{ij} n_j \quad (4)$$

where  $n_j$  are the direction cosines (cosines of the angles  $\mathbf{n}$  makes with each of the three principal axes) and  $\underline{\sigma}$  is what is known as a symmetrical ( $\sigma_{ij} = \sigma_{ji}$ ) second-rank *tensor*, known as the *stress tensor*, with nine elements ( $i = 1-3, j = 1-3$ ). For any surface element, the *normal stress* (force per unit area) is

<sup>7</sup>J. Krogh-Moe, *Acta Cryst.* **18** (1965) 77; *Phys. Chem. Glasses* **6** (1965) 46.

<sup>8</sup>P. J. Bray and J. G. O'Keefe, *Phys. Chem. Glasses* **4** (1963) 37.

<sup>9</sup>C. M. Kuppinger and J. E. Shelby, *J. Amer. Ceram. Soc.* **68** (1985) 463.

<sup>10</sup>W. Vogel, *Chemistry of Glass* (American Ceramic Society, Columbus, OH, 1985), pp. 101-109.

<sup>11</sup>L. W. Hobbs, “Mechanical properties of refractory oxides,” in: *Physics and Chemistry of Refractory Oxides*, ed. P. Thévenard (Sitjoff and Noordhof, Leiden, 1982). See also ***General Bibliography***.

$$\sigma_n = \sum_{i=1}^3 F_i n_i . \quad (5)$$

The resolved forces  $F_i$  cause atom displacements  $u_j$  along axes  $x_j$ .

Defining  $e_{ij} \equiv \partial u_i / \partial x_j$ , incremental displacements can be written as

$$du_i = e_{ij} dx_j \quad (6)$$

for small displacements  $du_i$ . The  $e_{ij}$  comprise the elements of a second-rank asymmetrical tensor  $\underline{\epsilon}$ , called the *infinitesimal strain tensor*, which is a measure of both rigid body rotation

$$\omega_{ij} = 1/2 (e_{ij} - e_{ji}) \quad (7)$$

and the pure strain (displacement per unit length)

$$\varepsilon_{ij} = 1/2 (e_{ij} + e_{ji}). \quad (8)$$

The strains  $\varepsilon_{ij}$  comprise the elements of a symmetrical second-rank tensor  $\underline{\epsilon}$ , called the strain tensor. If the strain is referred to the principal axes,

$$\underline{\epsilon} = \begin{vmatrix} \varepsilon_{11} & 0 & 0 \\ 0 & \varepsilon_{22} & 0 \\ 0 & 0 & \varepsilon_{33} \end{vmatrix} ; \quad (9)$$

for *uniaxial* strain along axis  $x_1$ , the strain tensor simplifies to  $\underline{\epsilon} = \varepsilon_{11} = e_{11} = \partial u_i / \partial x_1 \approx u/x_1$  for small displacements  $u \ll x_1$ .

For small strains in a body, the stress at any point is more or less linearly related to the strain, because the interatomic force-separation relationship is sensibly linear. This linear elastic behavior is approximated macroscopically in most solids, though the continuum approach can break down at the atomic level. Linear elastic behavior is just a generalized form of Hooke's law, which can be written

$$\sigma_{ij} = \sum_k \sum_l c_{ijkl} \varepsilon_{kl} \quad (10a)$$

or, more compactly,

$$\underline{\sigma} = \underline{\mathbf{C}} \underline{\epsilon} \quad (10b)$$

where  $c_{ijkl}$  are the elastic *stiffness constants* forming elements of the stiffness matrix  $\underline{\mathbf{C}}$ . Multiplying (10a) by the reciprocal  $c_{ijkl}^{-1}$  produces the equivalent relation

$$\varepsilon_{ij} = \sum_k \sum_l s_{ijkl} \sigma_{kl} \quad (11)$$

where  $s_{ijkl} = c_{ijkl}^{-1}$  are called the elastic *compliances*, which comprise the compliance matrix  $\underline{\mathbf{S}}$ . In their most general forms,  $\underline{\mathbf{C}}$  and  $\underline{\mathbf{S}}$  contain 81 terms each. Crystal symmetries, reflected in these matrices, dramatically reduce the number of elements; for a *cubic* crystal, for example, the elements are reduced to three constants,  $c_{11}$ ,  $c_{12}$  and  $c_{44}$ . For an elastically *isotropic* crystal (properties the same in all directions), only two elastic constants are required, since then

$$c_{44} = 1/2 (c_{11} - c_{12}). \quad (12)$$

The same is true of an isotropic *non-crystalline* material, though the axial labels i,j can no longer be conveniently aligned along convenient crystalline directions, such as unit cell edges; most glasses come under this rubric, since their *average* properties are the same in any direction. This fact enables the behavior of a linearly and isotropically elastic body to be entirely described by two more recognizable constants, *Young's modulus*  $Y$  and *Poisson's ratio*  $\nu$ , with

$$\begin{aligned} Y &= 1/s_{11} \\ \nu &= -s_{12}/s_{11}. \end{aligned} \quad (13)$$

For a solid defined by orthogonal axes ( $x_1, x_2, x_3$ ), Poisson's ratio represents the ratio of *perpendicular* (radial with respect to the axis) to *axial* strains induced,

$$\nu = -\varepsilon_{\perp} / \varepsilon_{\parallel} \quad (14)$$

(e.g. stretch a rod and it gets thinner, push on a rubber ball and it gets fatter); it is partially a statement of volume conservation in a material of limited compressibility. Values of Poisson's ratio typically lie between 0.2 and 0.3, although some cellular solids (like cork) can have zero or even negative (!) Poisson's ratios. For a *uniaxially* applied stress  $\sigma_1$  (where  $\sigma_2 = \sigma_3 = 0$ ) in an isotropic solid, the resulting elastic strains parallel and perpendicular to  $x_1$  are

$$\begin{aligned} \varepsilon_1 &= \sigma_1 / Y \\ \varepsilon_2 &= \varepsilon_3 = -\nu \varepsilon_1 = -\nu \sigma_1 / Y. \end{aligned} \quad (15)$$

**2. Mechanical measurement of Young's modulus.** A simple mechanical procedure by which to measure Young's modulus is the three-point bending test, in which a length of the solid in beam, rod or fiber form is supported at two points separated by a distance  $L$  and loaded by a transverse force  $F$  midway in between. The elastic deflection  $\delta$  in the direction of the imposed load arises from an axial extension  $u$  of the rod and is therefore related to Young's modulus. The actual relationship is

$$\delta = F L^3 / 48 Y I, \quad (16)$$

where the *moment of inertia*  $I$  for a beam of height  $h$  (measured along the force axis) and width  $w$  (perpendicular to the force axis) is given by

$$I = w h^3/12 ; \quad (17)$$

for a rod or fiber of ellipsoidal cross-section, with major and minor radii  $a$  and  $b$ ,

$$I = \pi a b^3/4 \text{ or } \pi b a^3/4 , \quad (18)$$

depending on whether minor or major axis, respectively, is oriented along the direction of applied force. Young's modulus can therefore be deduced from the deflection and a knowledge of the rod or fiber cross section. The maximum (axial tensile) stress in the rod or fiber is

$$\sigma_{\max} = F^2 L^4 / 96 Y I^2 . \quad (19)$$

Continuum elastic response of solid represents a uniform correlated motion of the constituent atoms (all the atoms respond in the same way: for example, all the atoms move closer together under hydrostatic compression). There are two cases of interest when atoms move less dependently of each other: when a displacement wave passes through the solid (sound, phonon propagation), and when atoms locally perform oscillatory motions with respect to each other in the absence of an external perturbation (*e.g.* thermal vibrations).

**3. Sound propagation.** Sound is a longitudinal mechanical pressure ( $P$  = force/unit area) wave<sup>12</sup> that can be approximated by propagation of a uniaxial stress pulse. For sound propagation in an (isotropic) liquid, necessarily contained by walls, the relevant materials properties are the compressibility

$$\kappa \equiv -V^{-1} \partial V/\partial P = \rho^{-1} \partial \rho/\partial P , \quad (20)$$

or its reciprocal, the bulk modulus  $B \equiv -V \partial P/\partial V = 1/\kappa = \rho \partial P/\partial \rho$ , and density  $\rho$ . The sound propagation velocity is given by

$$v_s = \sqrt{(B/\rho)} . \quad (21)$$

For an isotropic solid, where expansion or compression can take place perpendicular to

---

<sup>12</sup>Allan D. Pierce, *Acoustics: An Introduction to its Principles and Applications* (Optical Society of America, Melville, NY, 2005)

the propagation axis through the Poisson effect, the relevant materials are analogously Young's modulus and density, and the propagation velocity of an acoustical pulse is given by

$$v_s = \sqrt{Y/\rho}. \quad (22)$$

Since typical mechanical moduli for strongly-bonded solids (metals, ceramics) are in the 50 GPa range with densities  $\sim 1-10 \times 10^3 \text{ kg/m}^3$ , sound velocities in these solids are of order  $v_s \sim 5000 \text{ m/s}$ . Measurement of the speed of sound in a solid thus provides another convenient way to obtain its Young's modulus.

### Fracture

Most materials deform elastically under an applied stress up to a limit, called the *elastic limit*, and then revert to one of two further responses: 1) They fracture without further deformation. We call such a response brittle fracture and the material is classified as *brittle* (think teacup or window pane). Fracture occurs when new surfaces are created: the material breaks into two pieces, with the opposing surfaces created separating. 2) They continue to deform, but if the stress is released, the strain is not completely recoverable. We call such a response *plastic* (or permanent) *deformation*, and say that the material exhibits plasticity. Most plastic materials become increasingly harder to deform the more they are plastically deformed; this is known as work hardening (try bending a copper wire or pipe repeatedly) and implies that, at a constant stress, further deformation will eventually cease. A few materials (such as materials with sub-micrometer grain size) continue to deform plastically—in some cases, almost indefinitely—under a constant stress; this behavior is known as *superplasticity*. If the plastic deformation occurs at high temperature, material transport by atomic diffusion—for example by migration of point defects (such as vacancies)—may be responsible, occurring in a direction biased by the applied stress; this response is known as *creep*. Almost every material, whether it exhibits no plasticity or extensive plasticity and creep, will eventually fail by some kind of fracture process that creates new surfaces that separate. There are several modes of fracture, involving both normal and shear stresses. The easiest to envisage is simple tensile fracture (mode I) where the material breaks into two opposing pieces when it is pulled.

**1. Fracture Strength.** The maximum normal strain for an isotropically elastic body subjected to a uniaxial stress occurs across a plane normal to the stress axis. One might expect such a body to fail by fracture across this plane when subjected to a sufficiently large tensile force that the sum of the individual binding forces  $F_b$  exerted by atoms across this plane is exceeded. This will occur for a stress

$$\sigma_{th} = F/A \approx F_b n_A / a^2 n_A = (-dU_b/dr)_{max} / a^2 \quad (23)$$

where  $n_A$  is the number of atom pairs facing across the plane, whose interatomic spacing is  $a$ ,  $U_b$  is the bonding energy per bond of length  $r$ .  $\sigma_{th}$  is the theoretical tensile strength or *cohesive strength* of the solid. A reasonable estimate for  $\sigma_{th}$  can be made with some

knowledge of the interatomic bond energies (in covalent solids, from individual covalent bond energies, or in ionic solids from the summed Coloumb interaction between ions). Typical values yield

$$\sigma_{\text{th}} \approx Y/3. \quad (24)$$

An experimental estimate of the cohesive strength can usefully be made by recognizing that, during fracture, the stored elastic energy goes into creating new surfaces, each with specific surface energy  $\Gamma$ . The stored elastic energy is just the work done by the tensile force

$$W = Aa_0 \int^{\varepsilon} \sigma d\varepsilon = Aa \sigma^2 / 2Y, \quad (25)$$

where we have presumed Hookeian (ideal elastic) behavior to fracture. Assuming that fracture occurs reversibly and without dissipation of energy

$$W = 2 \Gamma A = Aa \sigma^2 / 2Y, \text{ or} \quad (26)$$

$$\sigma_{\text{th}} \approx 2(\Gamma Y/a)^{1/2}. \quad (27)$$

Values of surface energy  $\Gamma$  are not always well known, and (25) should include the uncertain contribution of dissipative processes (e.g. generation of heat, plastic flow, etc.) A value of  $\Gamma$  for many ceramic solids is  $\Gamma \approx 1 \text{ J/m}^2$ , which from (22) yields  $\sigma_{\text{th}} \approx Y/3$ . The force-distance curve for atomic bonding is not strictly Hookeian for large displacements, and (27) overestimates the cohesive strength. A better estimate, using more realistic force-distance curves, is

$$\sigma_{\text{th}} \approx (\Gamma Y/a)^{1/2} \approx Y/6 \quad (28)$$

**2. Fracture Mechanics.** In real materials, tensile fracture occurs at applied stresses far below  $\sigma_{\text{th}}$ , because real solids invariably contain imperfections or flaws which locally intensify the applied stress. Consider a sharp crack of length  $L$  and crack-tip radius  $\rho_c$ , extending through the solid normal to the applied tensile stress  $\sigma$ ; this could be a surface flaw or some extensive internal flaw. It was recognized by at least 1913 that the stresses at the end of a crack depend on the length of the crack, and that the presence of the crack locally intensifies the applied stress at the crack tip by a factor  $\{1 + 2\sqrt{(L/\rho_c)}\}$ . At a small distance  $x$  ahead of the crack, the stress in the crack plane is given by

$$\sigma_{ij} \approx \sigma \{1 + 2 [L/(\rho_c + 4x)]\}. \quad (29)$$

The intensification occurs because of the “lever arm” effect of the crack length  $L$ . The intensified crack-tip ( $x = 0$ ) stress (29) may exceed the cohesive strength (24), in which case the flaw extends at a minimum applied tensile stress

$$\sigma_f = (Y\Gamma\rho_c/4La)^{1/2} \quad (30)$$

and will lead to fracture if the extension is not checked or the crack tip blunted. The fracture stress (30) is a more general result than the usual Griffith<sup>13</sup> criterion

$$\sigma_f = (2 Y\Gamma/\pi L)^{1/2} \quad (31)$$

derived by equating the strain energy relieved by propagation of the crack to the resulting increase in surface energy. The two are equivalent for  $\rho_c = 3a$ , *i.e.* atomically-sharp crack tips, but (26) is more conveniently applied to fracture, since subsequent crack blunting in ceramics (*e.g.* by plastic deformation ahead of the crack) is small and can be entirely accounted for by adjusting  $\Gamma$  to include energy dissipated in plastic flow. Internal flaws can be treated with a small adjustment of  $L$ ; for example, a sharp penny-shaped crack of diameter  $d$  is given an effective value  $L = 4d(1 - v^2)/\pi^2$ .

The relationships (30) or (31) can be written

$$\begin{aligned} \sigma_f \sqrt{L} \cdot (8a/\rho_c)^{1/2} &= (2Y\Gamma)^{1/2}, \text{ or} \\ \sigma_f \sqrt{L} \cdot \pi^{1/2} &= (2Y\Gamma)^{1/2}. \end{aligned} \quad (32)$$

The left-hand side of eqn (32) should then be a *measurable* material parameter, called the *critical stress intensity factor*

$$K_{lc} = (2 Y\Gamma)^{1/2} \quad (33)$$

for the opening mode (mode I) of crack propagation. (There also exist two shear modes for crack propagation, modes II and III.) The crack will therefore advance when the stress intensity factor

$$K_I = \sigma \sqrt{(\pi L)} \quad (34)$$

achieves the value  $K_{lc}$ . The actual value of  $K_{lc}$ , which is also known as the *fracture toughness* (with units of MPa $\sqrt{m}$ ), will depend on the detailed state of the material (*viz* flaw population, configuration and distribution; porosity; plasticity; second phase barriers; and other microstructural variables), and therein lies its usefulness as a single parameter for characterizing fracture strength.  $K_{lc}$  is usually reasonably independent of temperature (following  $Y$  and  $\Gamma$ ), so the stress to extend inherent flaws should be roughly temperature independent also.

The great advantage of testing drawn glass fibers is that the surface of the glass fiber is very smooth and has not been disturbed by any external mechanical agent. This means that the surface flaw size is very small. Because the glass is quite homogeneous, there are no internal flaws or discontinuities (unless some internal crystallization—called *devitrification*—has occurred to create internal interfaces, like the grain boundaries in polycrystalline solids). Drawn glass fibers can thus exhibit remarkable fracture strengths, which is why they can be used so successfully in fiber optic cable applications.

---

<sup>13</sup>A.A. Griffith, “The phenomenon of rupture and flow in solids,” *Phil. Trans. Roy. Soc. (London)* **22** (1921) 163-198.

### **Experimental Procedure**

**1. Glass melting.** In this experiment, you will melt a series of eight alkali borate glasses with compositions 10, 15, 20, 23, 25, 28.5, 30 and 40 mol% Na<sub>2</sub>O. These will have been produced by reacting sodium carbonate (Na<sub>2</sub>CO<sub>3</sub>) with boric acid (H<sub>3</sub>BO<sub>3</sub>). Because the Na and B come from different reactants that are measured out separately by weight, it is common to represent the glass composition as RNa<sub>2</sub>O•B<sub>2</sub>O<sub>3</sub>, instead of by the alkali mole fraction M (*i.e.* as MNa<sub>2</sub>O•[1-M]B<sub>2</sub>O<sub>3</sub>), where the relative constituent oxide ratio R = M/(1-M) or M = R/(1+R). The stated mole fractions therefore correspond to R = 0.091, 0.176, 0.25, 0.30, 0.33, 0.40, 0.43 and 0.67. The two starting ingredients decompose on heating and reacting



accompanied by evolution of large volumes of (volatilized) gas that can lead to considerable foaming of the product until fully evolved. For this reason, the constituents were heated together slowly in a box furnace, beginning at 200 °C and increasing temperature by 100 °C increments every 30 minutes to 1000 °C. Because of time constraints, glasses of these compositions have been prepared in advance in 250 ml alumina crucibles, poured into smaller 50 ml alumina crucibles for ease of handling, and cooled. Nevertheless, as an exercise you should calculate the weights of each constituent required to produce the 50g or so of final product glass for each composition.

**2. Glass fiber drawing and the glass transition.** Reheat the crucibles and glass contents to 900 °C in a box furnace to remelt the glasses. Each melted product should, at 900 °C, be a low viscosity clear liquid without bubbles. Let the crucibles equilibrate for 15 minutes, then withdraw each crucible in turn with tongs and set it on an insulating brick. While one group member holds the hot crucible with tongs, another should take a ~200 mm length of 4-mm diameter vitreous silica rod and dip one end of the rod into the glass melt, withdrawing the rod *slowly* so as to draw out a glass rod or fiber at least 1.5-mm in diameter and 200-300 mm in length if possible. The drawing operation needs to be carried out slowly and at a critical viscosity (similar to that of honey or molasses), achieved over a small temperature range somewhat above T<sub>g</sub>, as the glass in the crucible cools. Drawing will stop rather suddenly when the melt cools significantly below this temperature range. Using diagonal cutters, cut the fiber near to the now-solidified melt surface and, when cool, break it off from the silica rod. You will want to draw at least two fibers of each composition and will need to reheat the crucible to 900 °C for 15 minutes between drawings. Keep fibers of different compositions separate in labeled trays or boxes. Make note of your qualitative impression of the comparative viscosities of each melt when first extracted from the furnace at 900 °C.

**3. Sound velocity, density and elastic modulus.** The rigidity of each borate glass composition will be assessed by measuring its mechanical response as characterized by its elastic modulus. This is most easily done by measuring the speed v<sub>s</sub> of sound (an

extensional wave) in the fiber, because for a purely axial compressional pulse Young's modulus  $Y$  for a glass of density  $\rho$  is given from (22) by

$$Y = \rho v_s^2. \quad (36)$$

The propagating compressional pulse, with rise time of  $< 1\mu\text{s}$ , is generated with a signal generator coupled to piezoelectric element attached to one end of the fiber, and its arrival is detected at the other with a second piezoelectric element. The time delay between sent and received pulses can be measured from oscilloscope traces of the piezoelectric potential(s), measured from the initial signal onset; from that delay and the accurately measured length of the fiber the pulse velocity can be deduced. The glass density can be measured by weighing the crucible and glass contents left over after fiber pulling, subtracting the previously measured weight of the empty crucible to get the mass of the glass, then filling the crucible with water and reweighing to get the volume of the glass remaining in the crucible. Alternatively, the glass fiber can be weighed and its volume estimated from its length and average diameter. Or, the supplied graph of density vs.  $\text{Na}_2\text{O}$  content may be consulted.

Plot the elastic modulus deduced against glass composition and use this information to establish where the maximum conversion from  $[\text{BO}_3]$  triangles to  $[\text{BO}_4]$  tetrahedra appears to have been effected before or at the same time as the alkali modifier begins to break up the network connectivity.

**4. Mechanical measurement of elastic modulus.** For each composition, select a portion of the drawn fiber of fairly uniform cross section and measure the major and minor ellipsoid diameters (optically, so as not to damage the surface of the fiber) at enough places along its length to establish reasonable averages for both. Place this uniform portion of each fiber in turn between the two pins of the three-point bending apparatus mounted on the light microscope stage, noting the orientation of major and minor ellipsoid axes. Slip the draw wire loop around one end of the fiber and slide to a central position precisely midway between the support pins. With the light microscope stage drives, center the fiber and obtain an image of the edge of the fiber on the video screen. Mark this edge with the cursor. Crank the neighboring translation table until a reading of 0.5 N-force is obtained on the spring balance attached to the pull wire and wire loop. Using the cursor, mark the new position of the edge of the fiber at its center and record the displacement. Release the stress by reversing the translation table crank until the displacement is zero, then reapply the 0.5 N force and ascertain repeatability.

Increase the spring balance load reading by 0.5 N-force intervals up to fracture (probably about 3-4 N, depending on fiber cross section), marking the new position of the edge of the fiber for each pull force. Plot the load against displacement to confirm elastic behavior and, using (16) and (18), calculate Young's modulus for each fiber in turn. Compare these results to those obtained from sound propagation velocities, and comment on the comparative uncertainties attending each method.

**5. Fracture strain and stress.** For each fiber, continue increasing the bending force until the fiber breaks. Just as the fiber breaks, note if possible the fiber displacement at the point of fracture (or, if not, at least record the translation table crank

dial setting) and the applied force at the instant of fracture (or at least the last recorded force sustained). Using (16) and (19), calculate the fracture stress and the strain at fracture. Assume a surface energy  $\Gamma = 1 \text{ J/m}^2$  and calculate the fracture toughness and the prevailing critical flaw size.

### **General Bibliography**

- Robert H. Doremus, *Glass Science* [2<sup>nd</sup> ed.] (Wiley, New York, 1994).
- E. J. Hearn, *Mechanics of Materials* [3<sup>rd</sup> edition], Volume 1: *An Introduction to the Mechanics of Elastic and Plastic Deformation of Solids and Structural Materials* (Elsevier, New York, 1997).
- W. David Kingery, H. K. Bowen and Donald R. Uhlman, *Introduction to Ceramics* [2<sup>nd</sup> ed.] (Wiley, New York, 1976).
- Brian R. Lawn, *Fracture of Brittle Solids* (Cambridge University Press, 1993).
- A. E. H. Love, *A Treatise on the Mathematical Theory of Elasticity* [4<sup>th</sup> edition] (Dover, New York, 1944).
- James E. Shelby, *Introduction to Glass Science* (Royal Society of Chemistry, London, 1993).
- Catherine J. Simmons and Osama H. El-Bayoumi, *Experimental Techniques of Glass Science* (The American Ceramic Society, Westerville, OH, 1993).
- Arun K. Varshneya, *Fundamentals of Inorganic Glasses* (Academic Press, New York, 1994).
- W. Vogel, *Chemistry of Glass* (The American Ceramic Society, Columbus, OH, 1985).